Remote Sensing of Environment 146 (2014) 63–76

Contents lists available at ScienceDirect

Remote Sensing of Environment

journal homepage: www.elsevier.com/locate/rse

Review

Challenges and opportunities for geostationary ocean colour remote sensing of regional seas: A review of recent results ☆

Kevin Ruddick [a,*], Griet Neukermans [a,1], Quinten Vanhellemont [a], Dominique Jolivet [b]

[a] Royal Belgian Institute for Natural Sciences (RBINS), Direction Natural Environment, 100 Gulledelle, 1200 Brussels, Belgium
[b] HYGEOS, Euratechnologies, 165 Avenue de Bretagne, 59 000 Lille, France

ARTICLE INFO

Article history:
Received 6 November 2012
Received in revised form 16 July 2013
Accepted 27 July 2013
Available online 16 October 2013

Keywords:
Geostationary
Ocean colour
Diurnal variability
Tidal variability
Data processing
Atmospheric correction

ABSTRACT

Ocean colour remote sensing from sun-synchronous polar orbiting satellites has become well-established as a tool for extracting information on phytoplankton and suspended particulate matter and related processes in regional seas. New data is now becoming available from optical remote sensors on geostationary satellites and provides a much higher temporal resolution, typically an image once or more per hour during daylight compared to once per day. This higher temporal resolution opens up obvious opportunities for dramatically improving the data availability in periods of scattered clouds and for resolving fast processes such as tidal or diurnal variability of phytoplankton or suspended particulate matter. As the science community starts to explore this new data source, further new applications are likely to emerge. However, the geostationary orbit presents also new algorithmic challenges. The coverage of high latitudes is limited by the difficulties of atmospheric correction at very high sensor zenith angle and ultimately by the earth's curvature. Exploitation of the new possibilities of viewing the earth for a range of sun zenith angles over the day also stimulates a need to perform accurate atmospheric correction at high sun zenith angle. Traditional pixel-by-pixel data processing algorithms could be supplemented by information on the temporal coherency of data over the day thus potentially improving data quality, by adding constraints to the inversion problem, or data quality control, by a posteriori analysis of time series. This review assesses the challenges and opportunities of geostationary ocean colour, with emphasis on the data processing algorithms that will need to be improved or developed to fully exploit the potential of this data source. Examples are drawn from recent results using data from the GOCI and SEVIRI sensors.

Contents

1. Introduction . . . 64
2. Ocean colour remote sensing systems and orbits . . . 64
   2.1. Near-polar sun synchronous orbits (SSO) . . . 64
   2.2. Geostationary orbit (GEO) . . . 65
   2.3. Geosynchronous orbit . . . 65
   2.4. Present and future GEO ocean colour missions . . . 66
   2.5. Possible GEO and SSO constellations . . . 67
3. GEO ocean colour data . . . 67
   3.1. Spatial and temporal resolution and coverage for SSO and GEO ocean colour . . . 67
   3.2. Viewing angles for SSO and GEO ocean colour . . . 68
   3.3. Spectral and radiometric characteristics for SSO and GEO ocean colour . . . 69
   3.4. Calibration and validation aspects for SSO and GEO sensors . . . 69
4. GEO data processing algorithms . . . 70
   4.1. New processes and algorithms . . . 70
   4.2. Atmospheric correction at high viewing and sun zenith angles . . . 70

* Corresponding author. Tel.: +32 2 773 2131; fax: +32 2 770 6972.
E-mail addresses: K.Ruddick@mumm.ac.be (K. Ruddick), gneukermans@ucsd.edu (G. Neukermans), Q.Vanhellemont@mumm.ac.be (Q. Vanhellemont), dj@hygeos.com (D. Jolivet).
[1] Now at: Marine Physical Laboratory, Scripps Institution of Oceanography, University of California, San Diego, La Jolla, CA 92093-0238, USA.

0034-4257/$ – see front matter © 2013 The Authors. Published by Elsevier Inc. All rights reserved.
http://dx.doi.org/10.1016/j.rse.2013.07.039

4.2.1. High total air mass . . . 71
4.2.2. Earth curvature — Rayleigh scattering . . . 71
4.2.3. Earth curvature — attenuation path length . . . 71
4.2.4. Fresnel reflectance . . . 71
4.2.5. Other high zenith angle processes . . . 72
4.2.6. Adjacency effects . . . 72
4.3. Multiscale algorithms for improving spatial resolution . . . 73
4.4. SSO + GEO synergy . . . 73
4.5. Exploiting temporal coherency . . . 73
4.6. Bidirectional effects . . . 74
5. Conclusions and future perspectives . . . 75
Acknowledgements . . . 75
References . . . 75

1. Introduction

Ocean colour remote sensing from polar orbiting sensors such as the Moderate Resolution Imaging Spectroradiometer (MODIS) and the MEdium Resolution Imaging Spectrometer (MERIS) has become well-established. Products for concentration of chlorophyll *a* and suspended particulate matter are widely used in marine science (McClain, 2009) and water quality monitoring (Bresciania, Stroppiana, Odermatt, Morabito, & Giardino, 2011). A single sun synchronous polar orbiting sensor (SSO) can provide global coverage. However, the sampling frequency, typically once per day, is too slow for resolving tidal and subdiurnal processes, particularly in coastal waters, and the presence of clouds is a big limitation to data availability. A single geostationary orbiting sensor (GEO) provides coverage of only part of the earth but offers a vastly improved sampling frequency, typically one image per hour, and hence the possibility to resolve new processes from space. This is illustrated in Fig. 1 where the tidal variability of suspended particulate matter is captured by data from the Spinning Enhanced Visible and Infrared Imager (SEVIRI) and is comparable to that found by in situ data, but is completely missed by the single image of MODIS-AQUA. The probability of obtaining data during periods of scattered clouds is also greatly enhanced, as shown in Fig. 1 (SEVIRI data for the North Sea) and Fig. 2 with data from the Geostationary Ocean Color Imager (GOCI) for the Bohai Sea. The difference between acquisition frequency for a typical SSO with overpass time at 12:30 UTC and a GEO is shown in Fig. 3, based on actual cloud-free observations of the Southern North Sea from SEVIRI. The simulated SSO sensor gives approximately 110 observation days per year compared to about 200 days/year for the GEO. Fig. 3 also shows the numbers of days/year, about 110 in this case, when four or more images would be available from a GEO with hourly acquisitions from 10:00 to 15:00, thus indicating the potential for resolving tidal processes.

However, the advantages go beyond simply obtaining more data. The exploitation of temporal coherency of natural processes offers entirely new ways of processing data — instead of pixel-by-pixel processing, information from adjacent pixels in time may allow better constraint of the ocean colour inversion problem or provide new opportunities for quality control via temporal outlier detection. Observation of a stable marine target over the day with different sun angles or the use of multiple geostationary sensors at different longitudes could give extra information on the bidirectional reflectance of the ocean–atmosphere system. Combination of high frequency geostationary data with empirical orthogonal function (EOF)-based multitemporal analyses methods, e.g. Beckers and Rixen (2003), can effectively fill gaps due to clouds and objectively identify outliers.

The objective of this paper is to present a review of the state of the art of geostationary ocean colour and to outline opportunities and challenges based on recent results from the GOCI and SEVIRI missions and analogous developments in other remote sensing fields (sea surface temperature, land and aerosols). This builds on the review made by the IOCCG (2012) and incorporates the findings of more recent studies in this fast-moving field. The particular focus of the present review is on coastal water applications, a priority niche for GEO exploitation as seen in the recent proliferation of studies of tidal variability of suspended particulate matter (Choi, Park, et al., 2014–this volume; Choi et al., 2012; Doxaran et al., 2014–this volume; He et al., 2013; Neukermans et al., 2009; Ruddick et al., 2012) and the related turbidity and diffuse attenuation (Neukermans, Ruddick, & Greenwood, 2012). The present review concentrates on aspects of data processing algorithms that are specific to GEO ocean colour.

A brief summary of the relevant SSO and GEO ocean colour satellite systems is given, highlighting the essential differences between the two orbits for data processing and exploitation. The impact of these differences on data processing algorithms is then assessed with some examples from new emerging methodologies. The new processes accessible to GEO are considered and the needs for corresponding new algorithms are outlined. The particular challenges of high zenith angle atmospheric correction are summarised. Multiscale algorithms, SSO/GEO synergy and algorithms using temporal coherency are addressed with reference either to early GEO ocean colour studies or to similar developments in other earth observation disciplines where GEO data exploitation is more mature. The challenges/opportunities regarding bidirectional effects are also summarised. Finally, the future perspectives for geostationary ocean colour are outlined.

2. Ocean colour remote sensing systems and orbits

In this section the satellite systems for ocean colour remote sensing are briefly described with a focus on the difference between the orbits for SSO and GEO. Table 1 gives some characteristics of two commonly-used SSO ocean colour sensors, MODIS and MERIS, and the first two GEO that have been used for ocean colour applications, SEVIRI (Schmetz et al., 2002) and GOCI (Ryu, Han, Cho, Park, & Ahn, 2012). Fuller details of these and many other past, present and future SSO ocean colour sensors, including the historically important Coastal Zone Color Scanner (CZCS) and Sea-viewing Wide Field of view Sensor (SeaWiFS), can be found at http://www.ioccg.org/sensors_ioccg.html. GOCI is the first (and, at the time of writing, the only) dedicated ocean colour sensor in geostationary orbit. SEVIRI is not designed for ocean colour applications, but has been included because of its demonstrated use for mapping suspended particulate matter and related quantities in turbid waters.

2.1. Near-polar sun synchronous orbits (SSO)

Near-polar sun synchronous orbits (SSO), sometimes termed "polar orbits", are a subset of the family of Low Earth Orbits (LEO), and have been adopted for nearly all ocean colour sensors to date, with the exception of the Hyperspectral Imager for the Coastal Ocean (HICO). SSO are typically 700–800 km above the earth's surface and a nadir-pointing SSO will cover approximately from pole to pole many times per day

with approximately constant mean local solar time for the equatorial overpass. A single wide swath SSO gives potentially full coverage of the earth's surface about once a day — exact frequency of acquisition depends on swath and latitude with greater overlap in acquisitions occurring at higher latitude. A typical coverage for SSO-based sensors is shown in Fig. 4, based on the MODIS-Terra and MODIS-Aqua sensors. The actual frequency of usable ocean colour data is reduced because of clouds, low quality data and/or sunglint. Sunglint is most critical in the tropics but might be reduced by along-track tilting of the sensor, as implemented for SeaWiFS, or by atmospheric correction algorithms specially adapted for low signal:noise conditions. For marine applications, viewing zenith angle for SSO is generally limited by design to optimise viewing conditions.

2.2. Geostationary orbit (GEO)

The angular speed of satellites in geostationary orbit is equal to the angular speed of the earth's rotation thus giving an effectively constant position above a location on the equator. This orbit, at the much higher altitude of 35,786 km, has long been used for telecommunications because it provides continuous coverage of locations within the area covered. However, in contrast to SSO, the maximal acquisition area of a single GEO is limited to part of the hemisphere centred on the equatorial sub-satellite point — in theory more than 40% of the earth's surface is visible from a single GEO, for which the satellite visibility at the sub-satellite point longitude extends up to 81° latitude (Robinson, 2004) for horizon viewing. In practice remote sensing at such high zenith angles is too difficult to achieve and, supposing that quantitative measurements are restricted to less than 60° zenith angle then good coverage of the earth's surface up to about 50° latitude is achieved with 5 GEO sensors — see Fig. 5. The limitation for high latitudes is critical and, as discussed later, a key challenge for the exploitation of GEO ocean colour is to develop better sensors and atmospheric correction algorithms that will push this limit as far as possible. Some early results for sensor zenith angles between 56° and 64° (Neukermans et al., 2012) have already shown that the "limit" of 60° zenith angle can be exceeded if the marine signal is strong enough.

Since the beginning of the Geostationary Operational Environmental Satellite (GOES) and the METEOrological SATellite (METEOSAT) series of satellites in the mid-1970s, the meteorological community has longstanding experience in the design and exploitation of geostationary sensors for the high frequency sampling of rapid processes such as the movement of clouds. The oceanographic community is beginning to recognise the important advantages offered by the geostationary orbit, firstly for sea surface temperature applications (Robinson, 2004) and more recently for ocean colour applications. These ocean colour applications present significant challenges because of the relative weakness of the marine reflectance signal as compared to the atmospheric reflectance, which must be accurately removed.

2.3. Geosynchronous orbit

The geostationary orbit is a special case of a circular geosynchronous orbit above the earth's equator. The more general class of geosynchronous orbits have an orbital period equal to the earth's rotation period,

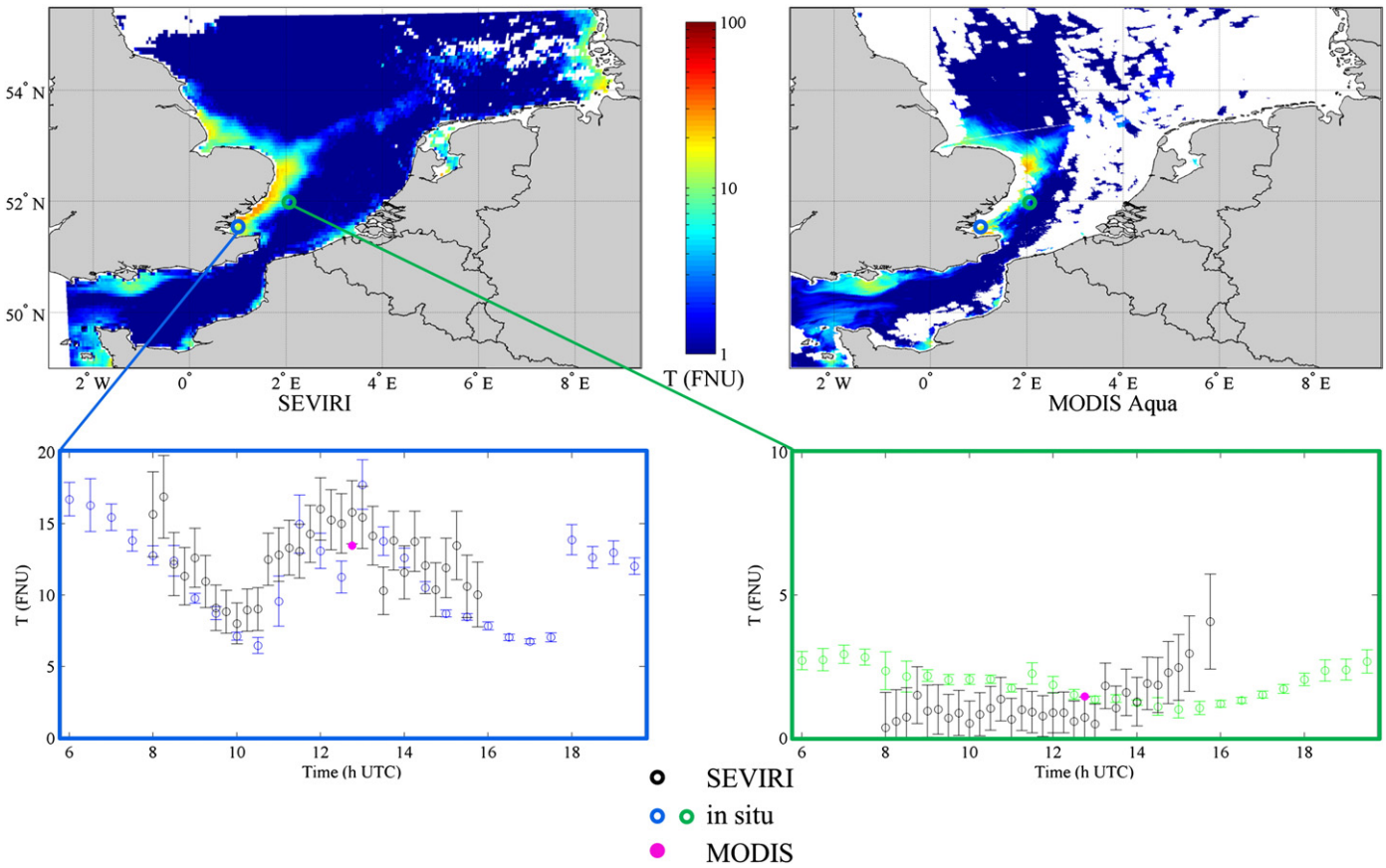

Fig. 1. Comparison of turbidity data derived from SEVIRI and MODIS-AQUA on 15th April 2008 using the processing of Neukermans (2012): (top-left) daily average from 34 SEVIRI images, (top-right) single MODIS-AQUA acquisition at 12:45 UTC. Corresponding time series of in situ and remotely sensed turbidity at (bottom left) the mouth of the Thames river (51.5235°N, 1.0240°E) and (bottom right) further offshore (51.9802°N, 2.0828°E). In the time series, SEVIRI data is given as grey dots, in situ optical data is given as blue or green dots according to location, and MODIS data is given as a single magenta dot for each location.) Full details of processing, including definition of the uncertainty bars for SEVIRI and in situ data, are given in Neukermans (2012) and Neukermans et al. (2012).

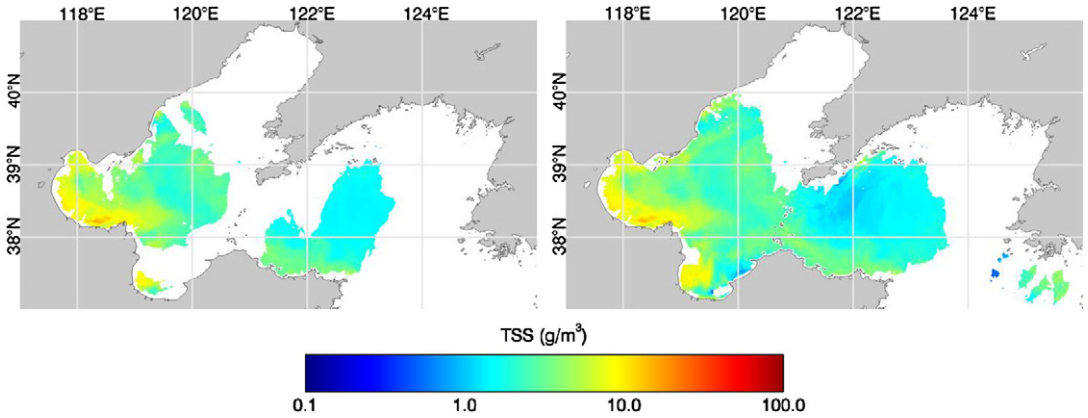

Fig. 2. GOCI Total Suspended Solids (TSS) data for the Bohai Sea from (left) single image acquired on 12.6.2011 at 05:16 UTC near overpass time of MODIS-AQUA and (right) daily composite mean average for the same day of up to 8 images over day, showing an example of the improvement in data quantity with multiple acquisitions per day. Redrawn from Ruddick et al. (2012) with kind permission from Springer Science and Business Media © Springer.

but the orbital plane may be inclined to the equator, giving a ground track which oscillates North and South of the equator during the day. This allows some viewing of higher latitudes, although this is achieved at the expense of some data in the other hemisphere, e.g. while the satellite is North of the equator, it is possible to view higher Northern latitudes but the higher Southern latitudes are then not observed. A non-geostationary geosynchronous orbit also loses the potential advantages of a constant viewing geometry. These orbits and the capabilities for better coverage of high latitudes are discussed in detail in IOCCG (2012), but are not considered further in this review because there are no immediate plans for launching such a mission.

2.4. Present and future GEO ocean colour missions

The only GEO ocean colour sensor currently in space is the GOCI sensor (Ryu et al., 2012). GOCI was launched in June 2010 and covers the Korea/China/Japan region with up to 8 images/day with spatial resolution of 500 m at (130°E, 36°N). Early results from GOCI are very promising and a summary of algorithms, calibration, validation and some preliminary applications can be found in Ryu and Ishikaza (2012) and the accompanying papers in that journal special issue edition.

As regards future GEO missions, the most mature plans at present are for GOCI-2, which has a projected launch date of 2018. In the USA, early plans for a geostationary ocean colour mission focussed on a Coastal Waters Hyperspectral Environment Suite (HES-CW) which was suggested for hosting by the Geostationary Operational Environmental Satellite (GOES-R), but subsequently cancelled. Plans are now focussed on the GEOstationary Coastal and Air Pollution Events (GEO-CAPE) mission (NRC2007), which may be launched after 2020. In Europe, some early studies have been carried out for a mission, named Geo-Oculus, with capabilities including ocean colour applications at a spatial resolution ranging between 20 m and 100 m. In France, further ideas for geostationary ocean colour missions have been proposed, named Ocean Colour Advanced Permanent Imager (OCAPI) and the Hosted Ocean Colour Imager (HOCI). Most of these dedicated geostationary ocean colour missions are many years away from reality or are even quite uncertain. More details of these missions can be found in IOCCG (2012).

In addition, a number of geostationary sensors not designed for ocean colour may have some limited utility. Of these, the Flexible Combined Imager (FCI) sensor, due for launch aboard METEOSAT

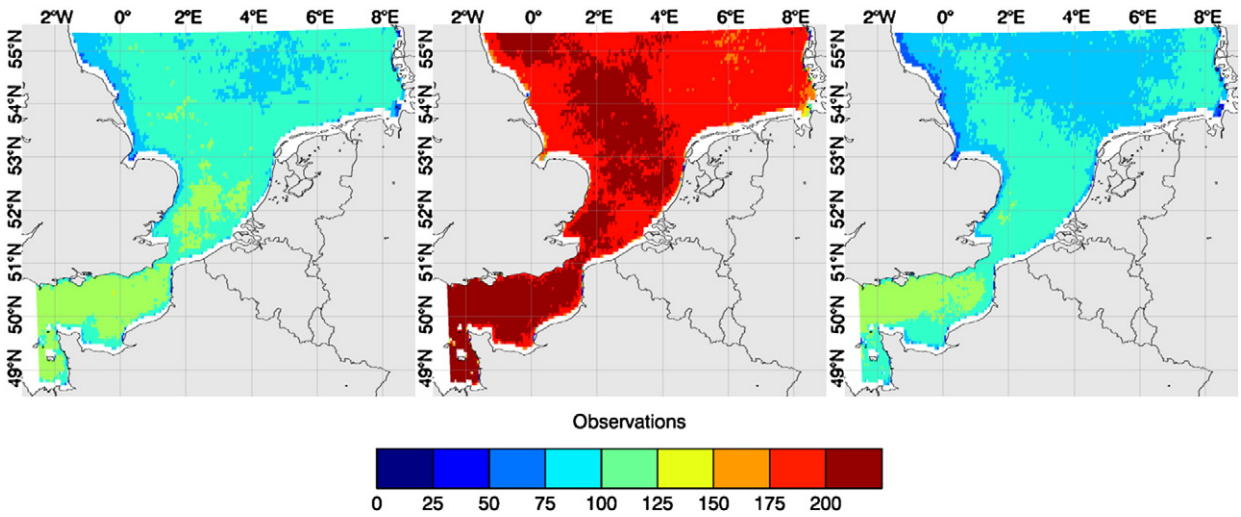

Fig. 3. The number of days in 2008 where valid data was obtained for SEVIRI observations of suspended particulate matter using the processing chain of Neukermans et al. (2012), but with an updated cloud masking procedure, and considering days where (left) the 12:30 UTC SEVIRI image gave valid data, (middle) any SEVIRI image during the day gave valid data, (right) at least four out of the six hourly images for 10:00–15:00 gave valid data. The latter simulates the potential for resolving tidal processes for a sensor with hourly acquisitions.

Third Generation Imager satellite (2016/2017), is the most promising. FCI should be superior to SEVIRI in a number of ways: a) the addition of blue (0.44 μm) and green (0.51 μm) bands, b), an improved spatial resolution of 500 m at nadir for the red (0.64 μm) band over Europe, c) addition of Short Wave Infrared bands at 1.38 μm and 2.25 μm which might be useful for atmospheric correction (if noise is sufficiently low), d) improved temporal resolution of 10 min for the full disc and 2.5 min for Europe and e) improved radiometric performance. Application of FCI in turbid waters to remote sensing of SPM and related parameters such as turbidity and diffuse attenuation of PAR is thus quite probable on the basis of experience with SEVIRI (Neukermans et al., 2009, 2012). Application of FCI in turbid waters to remote sensing of chlorophyll a seems infeasible because of the lack of spectral bands for red chlorophyll a absorption and fluorescence (660–690 nm). Application of FCI to remote sensing of chlorophyll a and/or diffuse attenuation coefficient in "Case 1" (Morel & Prieur, 1977) open ocean waters is an open question. The 0.44 μm and 0.51 μm bands certainly contain information relevant to chlorophyll a concentration (Morel & Maritorena, 2001) in such waters. The spectral resolution of FCI is far from the "minimum" requirements specified for an ocean colour sensor by International Ocean Colour Coordinating Group (IOCCG) (1998). The adequacy of the radiometric performance of FCI is also unclear, although it is noted that the high temporal resolution could be degraded significantly in post-processing, e.g. by suitable binning/averaging from 2.5 min to 1 h, to improve signal:noise ratio.

Other existing GEO meteorological sensors with at least two red/near infrared spectral bands and hence a (very) theoretical capability of remote sensing of SPM in turbid waters include MSU/Elektro-L1 (Russia), INSAT-3A-CCD (India) and FY-2CDE (China). At present, there are no known applications of these sensors to ocean colour problems. However, it is interesting to note that in the turbid waters of the Northeast Persian Gulf and the Gulf of Kutch, the INSAT-3A-CCD aerosol maps in Figure 2 of Sanwlani, Chauhan, and Navalgund (2011) show Angstrom exponent exceeding 1.0 and relatively stable in time. Since these maps were derived using an assumption of zero near infrared water-leaving radiance, it can be expected that turbid waters will contaminate the aerosol Angstrom exponent product in such a way, suggesting that INSAT-3A-CCD is detecting turbid waters.

2.5. Possible GEO and SSO constellations

While single sensor GEO missions can provide data for a single region, such as Europe and Africa as shown in Fig. 6, it is necessary to deploy a constellation of GEO missions to provide global coverage of tropical and temperate latitudes (excluding polar regions). Such a GEO constellation has theoretically been available since the 1990s for meteorological applications. However, owing to the typically regional nature of GEO missions, giving differences in instrument design, calibration and data distribution there are only a few examples of homogeneous global datasets, e.g. Knapp et al. (2011) for general climate studies and Freitas et al. (2013) for land surface temperature. Govaerts, Lattanzio, Taberner, and Pinty (2008) describe the consistent global merging of meteorological GEO data for surface albedo applications.

The deployment of a SSO constellation with different overpass times would improve the temporal resolution over a single SSO sensor for cloud avoidance. Very careful inter-calibration of the sensors would be required for quantification of high frequency temporal variability.

Of course, in practice design decisions regarding both single sensor and constellation missions will need to take account also of cost considerations. Mission cost is a complex matter beyond the scope of the present review, but it suffices to say that a single GEO mission is generally more expensive than a single SSO mission with similar sensor weight.

3. GEO ocean colour data

In this section the specificities of GEO ocean colour data will be summarised, in terms of differences with the more well-known SSO data.

3.1. Spatial and temporal resolution and coverage for SSO and GEO ocean colour

The most obvious differences between the SSO and GEO are in terms of temporal resolution and spatial coverage, as described above. High spatial resolution is more difficult to achieve, in engineering terms, from the higher GEO altitude because of the consequently greater requirements for optical magnification and pointing stability (Yang & Song, 2012). Edge of disk pixel distortion and degradation of spatial resolution is a permanent problem for high latitude GEO remote sensing. For example, a spatial resolution of 1.0 km at 0° latitude becomes approximately 1.5 km, 2.0 km and 2.9 km respectively at 40°, 50° and 60° latitude along the satellite longitude for a sensor with constant instantaneous field of view.

Table 1
Main characteristics of four satellite remote sensors that have been used for ocean colour applications. For a more exhaustive list of sensors, or more details on these, see www.ioccg.org and the links therein. VIS denotes number of visible bands (400–700 nm), NIR denotes number of near infrared bands (700–1000 nm), SWIR denotes number of short wave infrared bands (1 μm–3 μm) and TIR denotes number of medium and thermal infrared bands (3 μm–15 μm).

	AQUA-MODIS	ENVISAT-MERIS	MSG-SEVIRI	GOCI
Type	Ocean colour SSO	Ocean colour SSO	Meteorological GEO	Ocean colour GEO
Duration	2002+	2002–2012	2004+	2010+
Temporal resolution	Approximately: a) daily at 0°, b) twice per day at 50°N (if no loss owing to sunglint or edge of swath data)	Approximately: a) every 3 days at 0° b) every 2 days at 50°	15 min continuous (5 min for Europe)	Hourly
Temporal coverage	~1:30 PM LST equator crossing	~10:00 AM LST equator crossing	Continuous day/night	Up to 8 images/day 00:15–07:15 UTC
Spatial resolution	1 km at nadir (some land bands 250 m)	300 m at nadir	3 km * 3 km at (0°N,0°E) 3 km * 6.5 km at (52°N, 0°E) HRV band: /3	500 m at (130°E, 36°N) 360 m at nadir (0°, 128.2°E)
Spatial coverage	2330 km swath global	1150 km swath global	Full disc from 0°E (MSG-2) or 9.5°E (MSG-1)	~2500 km * 2500 km
Sun zenith	<70° processing	<70° processing	Limit not specified	Limit not specified
Sat zenith	<60° processing	<40.7° sensor	Limit not specified	<55° sensor
Spectral resolution	10 VIS, 6 NIR, 3 SWIR, 17 TIR	8 VIS, 7 NIR	2 VIS, 1 NIR, 1 SWIR, 8 TIR	6 VIS, 2 NIR
Sensor weight	229 kg	209 kg	270 kg	83 kg

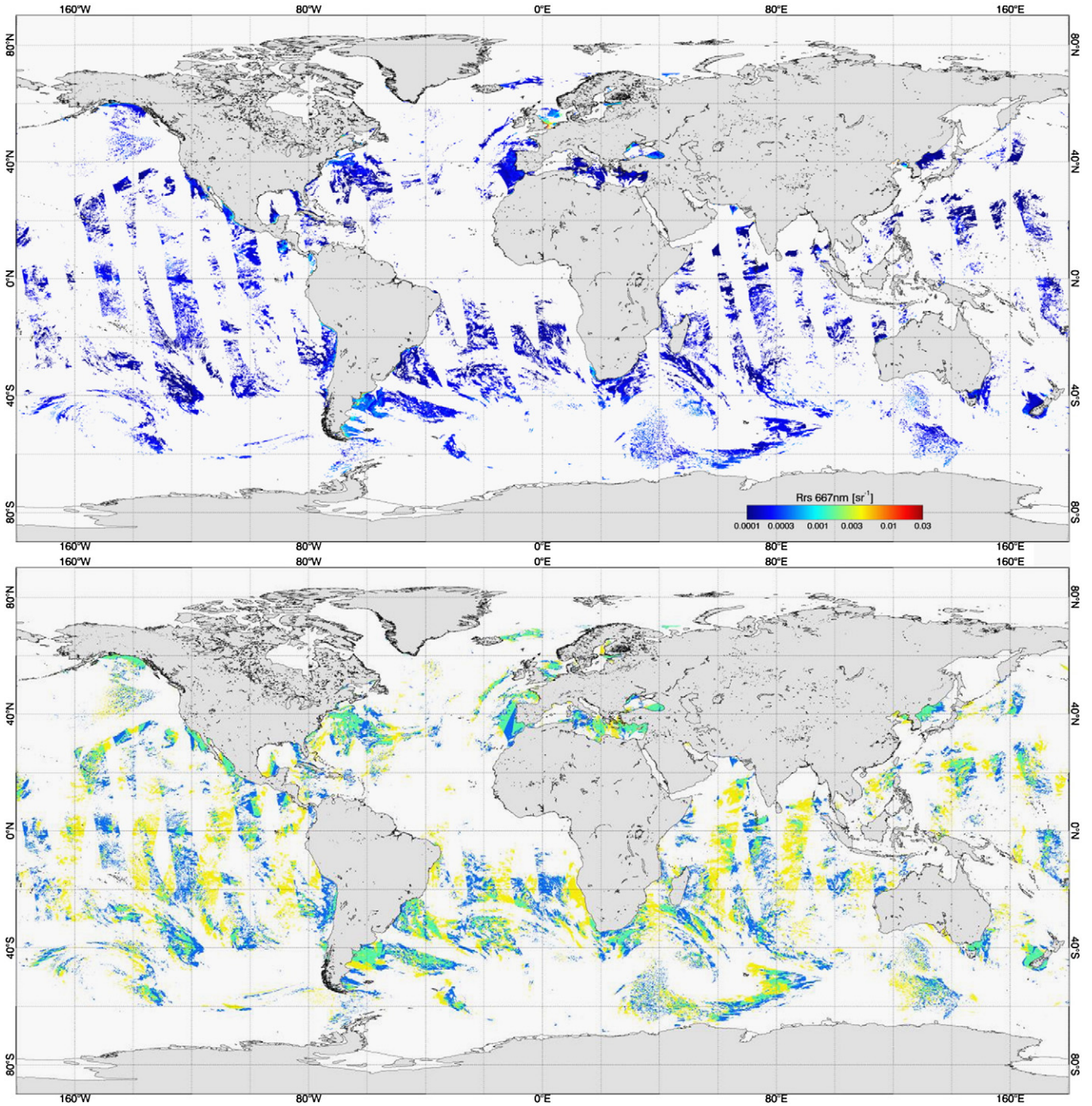

Fig. 4. Typical daily coverage for a SSO ocean colour sensor, as illustrated for 20.3.2012 by (top) MODIS-Aqua data and (bottom) a composite of MODIS-Aqua and MODIS-Terra data with local solar equatorial overpass times of respectively 13:30 and 10:30. In the top figure the colours are coded according to remote sensing reflectance at 667 nm. In the bottom figure blue regions show data from Aqua only, yellow regions from Terra only and green regions show data from both Aqua and Terra. In white areas data is missing because of clouds or other quality issues, especially sunglint, which is responsible for the north–south elongated white areas in the tropics.

3.2. Viewing angles for SSO and GEO ocean colour

One important additional difference in the orbits is the consequently different viewing (sensor) and sun zenith angles. These angles are often represented by the viewing and sun "air masses", given approximately by the secant of the respective zenith angle. These two components may be summed to give total air mass, which is equal to 2 for zenith sun and nadir viewing and increases, for example to 4 for sun and sensor zenith angles of 60°. The performance of atmospheric correction algorithms is often directly related to air mass (International Ocean Colour Coordinating Group (IOCCG), 2010) and high total air mass conditions may degrade greatly the data quality. This challenge may stimulate different data processing algorithms for GEO ocean colour as discussed in Section 4. For SSO sensors, viewing zenith angles are limited by design to avoid high air mass atmospheric correction problems. For GEO sensors, limitations on viewing zenith angle would critically reduce the

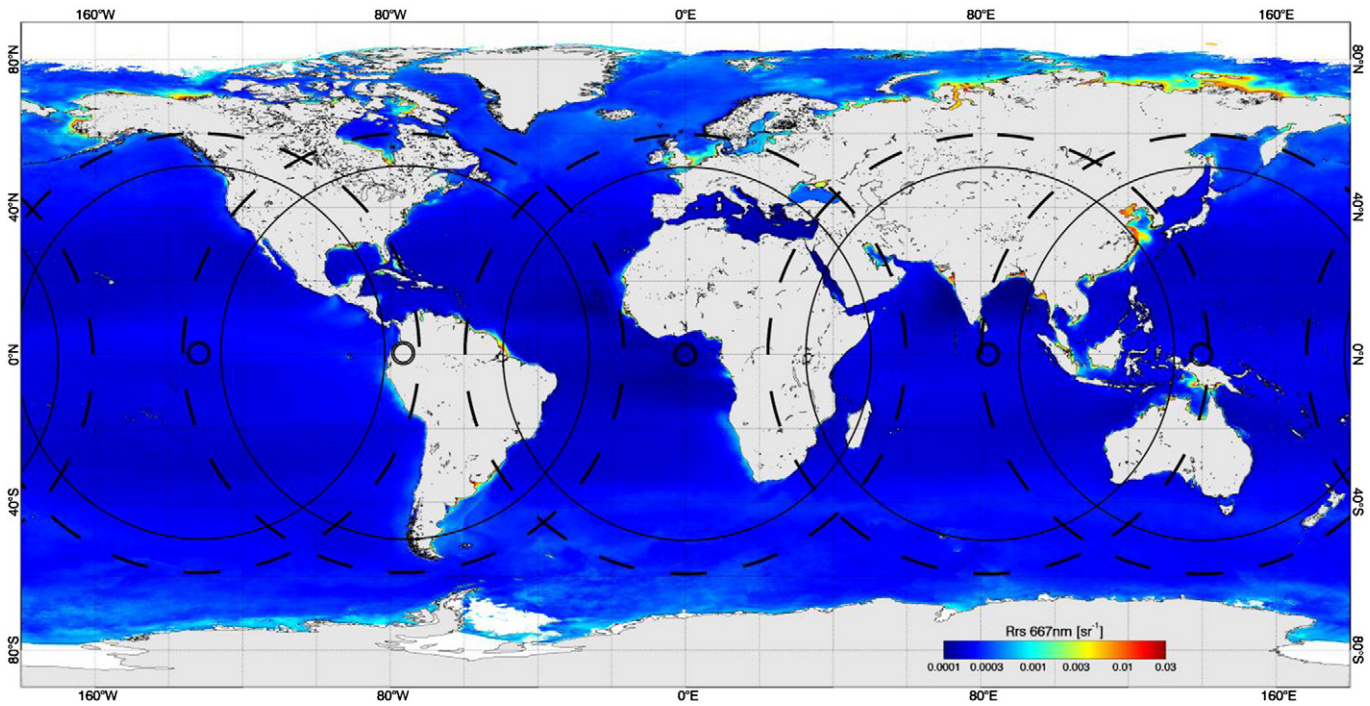

Fig. 5. Approximate ground visibility from five geostationary satellites, located above the equator as shown by small black circles. The dashed and solid line ellipses are bounded by sensor zenith angle of 60° and 70° respectively. The background image shows remote sensing reflectance at 667 nm from MODIS as a composite for the period of 1 July 2002 to 30 July 2012. The limiting sensor zenith angle for ocean colour SSO sensors is a key question for researchers and will depend on various factors (desired product accuracy, sun zenith angle, turbidity of water, atmospheric correction algorithm, etc.).

acquisition area and so there is a strong interest in pushing algorithms to deal with higher and higher viewing zenith angles as can be seen in Fig. 6.

Similarly whereas an optimally low sun zenith angle is adopted for most SSO sensors, the very advantage of high frequency data from a GEO implies the need to acquire observations for the more challenging high sun zenith angles. The variation of air mass and Rayleigh reflectance at 635 nm is shown over the day for a location in the Southern North Sea for the Northern summer solstice and autumn equinox in Fig. 7. Rayleigh reflectance varies with wavelength, λ, approximately as λ^{-4}, and so will be proportionally about 5.6 times larger at 412 nm.

A second important aspect of the viewing geometry, in this case advantageous, is that the viewing zenith and azimuth angles are constant in time for a GEO sensor over the day and over the year. There is not yet sufficient experience with GEO ocean colour data processing to determine whether/how this constant viewing geometry could be exploited, although it seems already likely that there will be advantages for sensor calibration and product validation, as described below.

3.3. Spectral and radiometric characteristics for SSO and GEO ocean colour

While a variety of engineering approaches are available for both SSO and GEO ocean colour sensors, the spectral and radiometric characteristics, as seen by the data user (ocean colour scientists in this context), can be quite similar and can be met by suitable engineering design. The requirements for spectral resolution are set by the target parameters, which are in turn set by the science questions and applications. For example, the need to remotely sense chlorophyll a concentration in clear and turbid waters triggers a need for a set of spectral bands which are common for both SSO and GEO. Similarly the radiometric sensitivity required for such an application is common to SSO and GEO operating at the same total air mass, even though this radiometric sensitivity may be achieved by very different engineering designs, e.g. using larger integration times for GEO data. Pushing GEO to higher total air mass situations will impose correspondingly more stringent constraints on radiometric signal: noise ratio.

3.4. Calibration and validation aspects for SSO and GEO sensors

Many aspects of the calibration and validation of ocean colour sensors apply to both SSO and GEO sensors, although very different engineering approaches may be adopted. For example, the SSO SeaWiFS sensor performed a moon calibration by tilting of the satellite, whereas direct viewing of the moon by simple enlargement of the viewing area is feasible for a GEO sensor. Summaries of ocean colour sensor calibration and validation are given by Barnes, Eplee, Schmidt, Patt, and McClain (2001), Franz, Bailey, Werdell, and McClain (2007) and Hooker and McClain (2000). The current section considers only the aspects where the orbit (SSO or GEO) makes an important difference.

The vicarious calibration of SSO ocean colour sensors may be carried out using stable land or sea targets, which are observed typically once per day. The aerosol contribution to top-of-atmosphere radiance must be estimated. For a GEO, if the aerosol type and concentration is constant over the day then the variation in sun angle over the day provides more information for the estimation and removal of this aerosol contribution, in a similar way to the use of Langley extrapolation for the calibration of ground-based sunphotometers (Shaw, 1983).

A second orbit-related aspect of sensor calibration is that the difference in viewing angle on different SSO overpasses will add uncertainty for non-Lambertian targets, but this will not be a problem for GEO observations. In a similar way, the uncertainty associated with bidirectional effects can be reduced for GEO observations used in validation activities.

More importantly as regards validation, the critical problem of insufficient matchups for validation of SSO ocean colour products is greatly reduced for the higher frequency GEO observations. For example, continuously measuring in water optical instruments can give many matchups per day for a GEO sensor, an order of magnitude better than for SSO sensors, as demonstrated for the validation of SEVIRI-retrieved

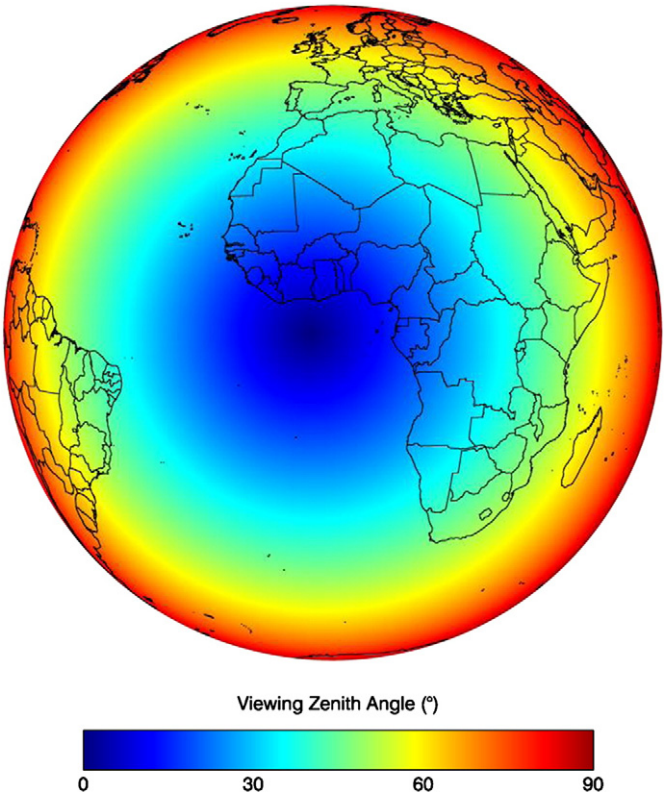

Fig. 6. Full disc of the SEVIRI sensor onboard the MSG1/METEOSAT-8 geostationary satellite, when located at 3.5°W, showing viewing zenith angle in degrees.

turbidity by Neukermans et al. (2012). A similar order of magnitude increase in the number of reflectance matchups from autonomous radiometer systems such as those of the AERONET-OC network (Zibordi et al., 2009) will be achieved when comparing GEO validation with SSO validation. In fact, the use of a GEO sensor may assist in the validation of SSO sensors, since it will be possible to evaluate temporal variability between the SSO acquisition and the in situ data acquisition and hence determine the associated uncertainty.

4. GEO data processing algorithms

The "level 2" (L2) processing of calibrated top-of-atmosphere radiometric data from polar-orbiting ocean colour sensors such as SeaWiFS, MODIS and MERIS can be decomposed into atmospheric correction, yielding bottom-of-atmosphere marine reflectance data and bio-optical model inversion yielding in-water optical properties, e.g. absorption or backscatter coefficients, diffuse attenuation coefficients, etc., or related biogeophysical parameters such as the concentration of chlorophyll a or suspended particulate matter. The atmospheric correction and bio-optical model inversion steps may be explicitly separated, as in the approach of Gordon and Wang (1994), or may be combined by the inversion of a coupled ocean–atmosphere system (Doerffer & Fischer, 1994). A high degree of generality has been achieved in the framework of the SeaDAS software (Fu, Baith, & McClain, 1998), which provides multi-mission processing of many ocean colour sensors using the same fundamental approach (flagging of invalid/suspect/extreme data, corrections for atmospheric gas absorption, molecular scattering and aerosol scattering, estimation of chlorophyll a from marine reflectances, etc.). Most mission-specific or research L2 processors adopt a similar pixel-by-pixel data processing approach and there is, in principle, no reason why the same approach cannot be adopted for geostationary ocean colour as has already been demonstrated by processing of SEVIRI (Neukermans et al., 2009) and GOCI data (Ahn, Park, Ryu, Lee, & Oh, 2012). So is the L2 processing of geostationary ocean colour data fundamentally the same as the processing of polar-orbiter ocean colour data with "just" more images per day? What are the new challenges and the new opportunities provided by geostationary ocean colour data and what new algorithmic approaches are needed to fully meet these challenges and exploit these opportunities?

In the following section, some ideas regarding processing algorithms specific to geostationary ocean colour data will be outlined with a focus on L2 processing. These ideas are summarised in Table 2 in terms of the different SSO/GEO characteristics described previously in Section 3.

4.1. New processes and algorithms

The new processes that could be resolved by high frequency data from GEO ocean colour will naturally stimulate the need for new algorithms to generate the most appropriate data corresponding to these processes. As a trivial example, tidal variability could be quantified using daily average and standard deviation, etc. Such processing is not conceptually different from similar multitemporal products generated at longer time scales, such as monthly or annual composites, described in detail in International Ocean Colour Coordinating Group (IOCCG) (2007). The timing of minimum/maximum concentrations in day or harmonic analysis of time series is also relevant for tidal processes. The estimation of daily primary production may be improved by the knowledge of (uncorrelated) variations of phytoplankton biomass and Photosynthetically Available Radiation (PAR) during the day (Lee et al., 2012). Abovewater PAR itself can be better estimated from GEO high frequency data (Frouin & McPherson, 2012). As regards underwater PAR, the difference between use of a daily mean PAR attenuation coefficient and the instantaneous PAR attenuation coefficient for waters with tidally-varying SPM concentration can be even more critical — daily-averaged phytoplankton growth will be much higher in the case where the moment of minimum PAR attenuation coincides with the moment of maximum abovewater PAR (Desmit, Vanderborght, Regnier, & Wollast, 2005).

Cloud clearing algorithms can range from simple multitemporal averaging to the more powerful techniques such as optimal interpolation or empirical orthogonal function based approaches (Sirjacobs et al., 2011) as are already used at longer time scale for SSO data.

Other new processes that could be resolved, e.g. involving the diurnal variation of light and photosynthesis-related parameters (Bruyant et al., 2005; Loisel et al., 2011; Stramska & Dickey, 1992) or the diurnal vertical migration of certain species (Kamykowski, 1981), will also require new algorithms. In these cases the necessary algorithmic research will be very process-specific and are more of the domain of marine bio-optics than of ocean colour data processing.

Choi, Yang, Han, Ryu, and Park (2013) suggest a method for estimation of ocean surface currents from the horizontal movement of suspended sediments.

Finally, hitherto unimagined new processes will probably emerge once high frequency data becomes available. As an example of an unexpected new application, Hong et al. (2012) report tracking of the hour-by-hour trajectory of a ship dumping sewage sludge, suggesting new perspectives for the monitoring of illegal maritime activities.

4.2. Atmospheric correction at high viewing and sun zenith angles

The atmospheric correction for high air mass conditions (high sensor and/or sun zenith angles) is a major challenge for geostationary ocean colour data. This is not fundamentally a new problem, because data, e.g. from MERIS and MODIS, is already acquired for high sun zenith angles at polar latitudes and at temperate latitudes in winter. This data is generally discarded via masking procedures as too difficult to process, but the data loss is not considered to be critical. However, the equatorial position of geostationary sensors means that sensor zenith angle is

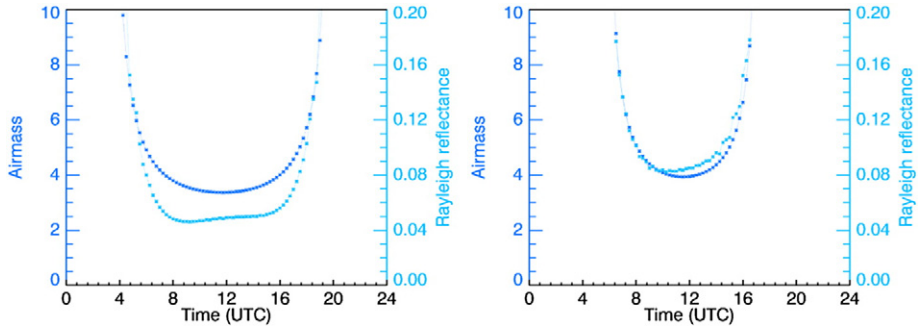

Fig. 7. Variation over day of total air mass (dark blue) and Rayleigh reflectance (light blue) at the 0.635 μm band for the SEVIRI sensor onboard MSG1-Meteosat8 (3.5°W) for a location in the Southern North Sea (55.0°N, 5°E). on 20th June (left) and 22nd September (right) 2012.
Rayleigh reflectance has been calculated according to Neukermans et al. (2012).

systematically high at high latitudes throughout the year. Moreover the possibility of exploiting data throughout the day with geostationary sensors will depend critically on any limit on acceptable sun zenith angle — this limit will be reached every day in every location and must therefore be pushed as far as possible. The difficulties of atmospheric correction for high sensor or sun zenith angles are multiple.

4.2.1. High total air mass

The atmospheric path radiance scales approximately in proportion to total air mass. Many atmospheric correction algorithms estimate directly the atmospheric path radiance, e.g. by calculation of Rayleigh reflectance from geometry and atmospheric pressure (Gordon, Brown, & Evans, 1988) and by calculation of aerosol reflectance in the near infrared (NIR) or Short Wave Infrared (SWIR) and extrapolation to shorter wave lengths using tabulated aerosol models (Gordon & Wang, 1994). These algorithms usually have an error that increases with total air mass, typically linearly, as shown in International Ocean Colour Coordinating Group (IOCCG, 2010) and as could be expected from simple considerations of marine: atmospheric reflectance ratio. The simulations of International Ocean Colour Coordinating Group (IOCCG, 2010) go up to a total air mass of just greater than 5.0, which is sometimes considered as a reasonable limit (International Ocean Colour Coordinating Group (IOCCG), 2010).

4.2.2. Earth curvature — Rayleigh scattering

At high zenith angles, greater than 70° according to Ding and Gordon (1994), the plane parallel assumption (PPA), used as a basis for all operational ocean colour atmospheric correction algorithms, is no longer valid and the earth's curvature must be considered, e.g. via the spherical shell approximation (SSA) (Wang, 2003). Computations based on the SSA are very time consuming, although some simplifying approaches may be adopted to achieve computationally efficient corrections to the PPA for high zenith angles. Adams and Kattawar (1978) note that the ratio of single-scattering radiance to total scattering radiance is nearly the same for a PPA model as for a SSA model under the same conditions. Ding and Gordon (1994) note the importance of calculating the Rayleigh scattering via a SSA and propose an efficient method for doing so.

4.2.3. Earth curvature — attenuation path length

Calculations for direct and diffuse atmospheric transmittance also need to be modified at high zenith angle and high optical thickness. As illustrated in Fig. 8, the geometrical distance from the earth's surface to the top of atmosphere is different from the path length used in PPA calculations. To our knowledge this has not been previously studied for ocean colour applications, although Spurr (2002) describes for atmospheric applications a pseudo-spherical approximation (PSA). In this PSA the atmospheric attenuation of the direct solar beam is calculated by integrating along the optical path, taking account of the secant at each altitude rather than just the secant at the earth's surface. In a PPA these secants are equal at all altitudes.

4.2.4. Fresnel reflectance

Further problems arise for high sun and sensor zenith angles because the Fresnel reflectance of the air–sea interface increases significantly for abovewater zenith angles greater than 45°. This is shown in

Table 2
Spatio-temporal, geometric and other aspects of SSO and GEO orbits and the consequent implications in terms of new challenges and opportunities for GEO ocean colour.

	SSO	GEO	GEO algorithm challenges/opportunities
Temporal resolution	~1/day	~1/h	New products and processes New temporal coherency QC or inversion constraints New daily composites and daily/tidal variability Possible SSO + GEO synergy Possible shift from pixel-by-pixel to time series processing
Temporal coverage	E.g. noon	Daytime	Need for high θ_0 atmospheric corr.
Spatial resolution	~250 m–1 km	~500 m–5 km High latitude and off-centre degradation	Multiscale algos Multisensor synergy algos
Spatial coverage	Global	Disc centred on equator up to 55° latitude? See Figs. 5 and 6	Need for high θ_v atmospheric corr. Possible dual view BRDF
Sun zenith	<70° (algo limit)	CHALLENGE	High θ_0 atmospheric corr. New BRDF correction/exploitation algos
Sat zenith	<60° (algo limit)	CHALLENGE Constant θ_v	High θ_v atmospheric corr.
Calibration	Prelaunch + onboard (sun/moon) + vicarious (land/sea)	As SSO + reduced BRDF and aerosol uncertainties for vicarious calibration?	Refine vicarious calibration
Validation	Matchup (+intersensor)	As SSO but matchups * 8 (including high air mass) Reduced BRDF uncertainty?	Refine with BRDF

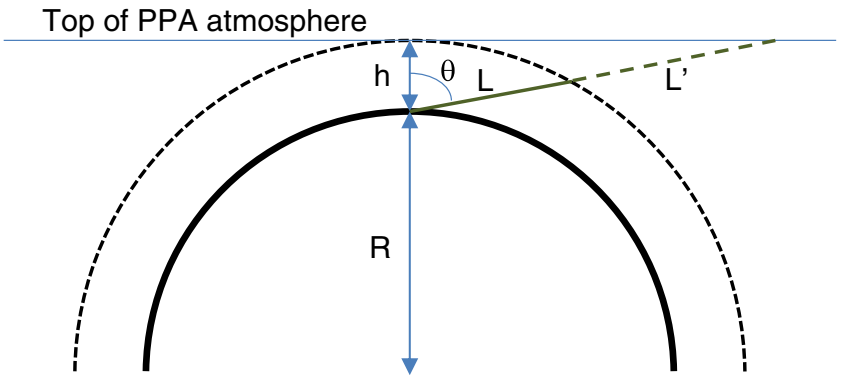

Fig. 8. Schematic view of the geometrical path lengths from earth surface, solid black line, to the top of atmosphere in a plane parallel approximation (PPA), thin blue line, and in a spherical shell approximation (SSA), dashed black line, for a planet with radius R and an atmosphere with (greatly exaggerated) height h. For SSA the geometrical path is shown by the solid green line, with length, L. For PPA the extra geometrical path is shown by the dashed green line, with length L′. The zenith angle, θ, can represent either the sun or the sensor zenith angle.

Fig. 9 where the reflectance of the interface is respectively 0.021, 0.022, 0.035 and 0.135 for abovewater zenith angles of 10°, 30°, 50° and 70°. This has three consequences in the geostationary perspective. Firstly, for high sensor zenith angle the reflected (Rayleigh and aerosol) skylight will become more significant, by a factor 6 at 70°, and will need to be more accurately removed. Secondly for high sun zenith angle, the reduction in interface transmittance must be accounted for, as studied in detail by Wang (2006). Thirdly, for high sensor zenith angle the water-leaving radiance will be reduced by in-water Fresnel reflection. This can be seen for viewing zenith angles greater than 70° in Figure 8 of Park and Ruddick (2005), although it was noted there that "such a large zenith is not generally appropriate for remote sensing".

4.2.5. Other high zenith angle processes

The questions raised by GEO ocean colour are quite new and it is possible that further aspects of atmospheric correction and air–sea interface correction may need refinement at very high zenith angles. The theoretical fundamentals were laid down in the 1970s and 1980s (Gordon, 1978; Gordon & Morel, 1983) when ocean colour remote sensing at high zenith angles seemed unimaginable. The many simplifying approximations made at that time may need to be fundamentally re-evaluated to check for consistency in high zenith angle applications. As an example the shading effect of surface waves may become important for high sun zenith angles as illustrated in Fig. 10.

4.2.6. Adjacency effects

Adjacency effects are already critical for nearshore and inland waters (Santer & Schmechtig, 2000; Sterckx, Knaeps, & Ruddick, 2011) and very difficult to correct for at moderate zenith angle. Adjacency effects will contaminate larger areas at high sun and sensor zenith angles as shown in Table 5 and Figure 13 of Santer and Schmechtig (2000) respectively.

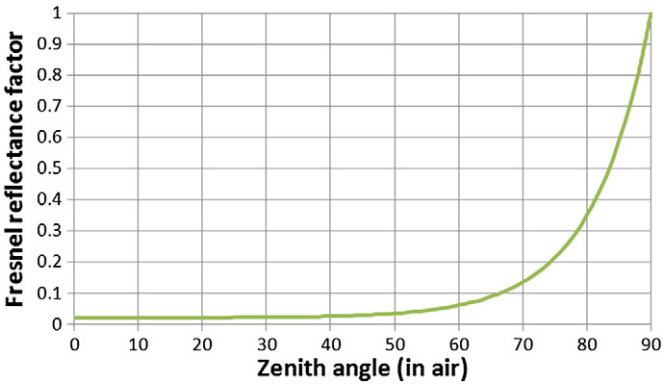

Fig. 9. The Fresnel reflectance of the air–sea interface as function of the zenith angle in air, calculated for a typical oceanic refractive index of 1.34. This reflectance factor is the same for light incident from air and light incident from the water side of the interface provided that the zenith angle is measured in air in both cases. Thus for diffuse skylight or direct sunlight incident on the air–sea interface at an incident zenith angle of 80°, about 35% is reflected at the interface back towards the sky/sensor. For water-leaving radiance emerging from the air–sea interface at a transmitted zenith angle of 80°, about 65% of the below-surface upwelling radiance is internally reflected back into the water. Calculations are shown here for a flat sea surface.
For a wind-roughened sea surface see Mobley (1994).

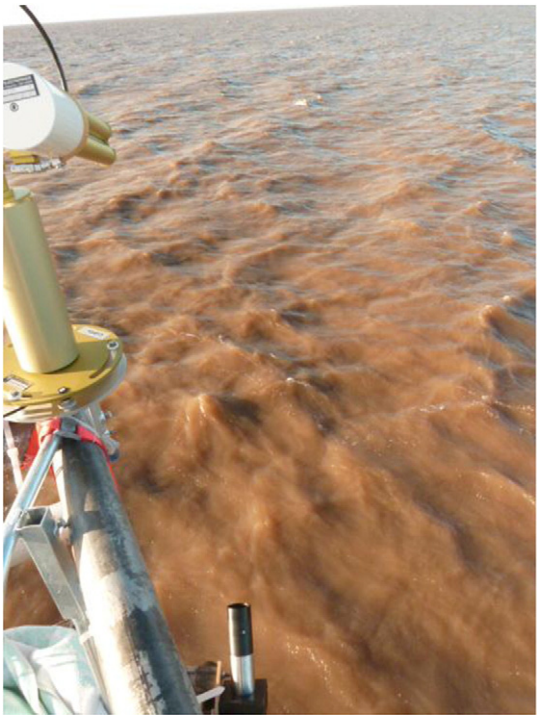

Fig. 10. Photograph of the surface taken in the turbid waters of the Rio de La Plata Estuary for a sun zenith angle of approximately 75° and low wind conditions with typical significant wave height of about 10–20 cm. The sun is to the left of picture and in the foreground radiometer systems are visible. Darkened areas of wave shadowing are clearly visible to the right of the larger wave crests.

4.3. Multiscale algorithms for improving spatial resolution

The difficulties of achieving high spatial resolution which are already challenging at the sub-satellite point from the geostationary orbit, but which are further exacerbated by high sensor zenith angles, may stimulate the development of new multiple length-scale algorithms. For SeaWiFS and MERIS all spectral bands were acquired at the same spatial resolution and L2 data processing naturally preserves the finest spatial resolution unless computational requirements imposes practical limits. MODIS was designed with ocean colour bands at 1000 m resolution, but with a few higher resolution (250 m or 500 m) bands designed for land/cloud/aerosol applications. Although not originally foreseen for such purposes, some algorithms (Hu et al., 2004; Miller & McKee, 2004) have been designed to take advantage of these higher resolution MODIS bands for mapping of marine suspended particulate matter. Thus, lower spatial resolution bands can be used for correction of aerosols (assumed to be constant over the larger pixels) and the higher spatial resolution bands can be used to capture small scale variations of SPM. Such an approach was adopted by Neukermans et al. (2012) to take advantage of the higher spatial resolution of the panchromatic High Resolution Visible (HRV) band of SEVIRI, although it is noted that the use of such a wide spectral band is not optimal for quantification of a range of SPM concentrations. Such multi-scale algorithms are not common in ocean colour, but are more widespread in other earth observation disciplines (Ehlers, 1991). Dedicated ocean colour sensors are not generally designed with different spatial resolutions for different spectral bands, and the use of multi-scale algorithms has to date been limited to exploiting the higher spatial resolution of bands designed for non-ocean colour applications.

4.4. SSO + GEO synergy

Synergistic use of SSO and GEO ocean colour data may offer new opportunities. Current studies with synergistic use of SSO ocean colour sensors have focussed particularly on the merging of long term datasets for chlorophyll for the purposes of studying climate change with the prime motivation being to overlap limited duration missions into a longer time series (International Ocean Colour Coordinating Group (IOCCG), 2007, 2010). There have been a limited number of studies to use multiple observations within a day to study high frequency variability, e.g. from AVHRR (Stumpf, Gelfenbaum, & Pennock, 1993). In such applications, intersensor matching of calibration and algorithms can be challenging, because uncertainties must be keep lower than the natural variability which is to be observed. In the new context of geostationary ocean colour data, there is a new motivation to consider synergistic use to exploit the high temporal resolution of geostationary and the (typically) high spatial resolution of polar-orbiters instead of the much costlier approach of aiming for high spatial and temporal resolution from the same instrument. This can be achieved for processes where space and time variability are essentially separable at least within the space/time scales considered, for example in the case of tidal vertical resuspension of bottom sediments, but not for processes such as horizontal advection where space–time variability is more complex. A preliminary study combining SEVIRI and MODIS-AQUA (Vanhellemont, Neukermans, & Ruddick, 2014–this volume) for the mapping of SPM in turbid waters has shown promising results, giving SPM maps every 15 min at 1 km resolution as shown in Fig. 11.

Synergistic use of SSO and GEO ocean colour data will be facilitated by the use of common spectral bands, e.g. following the recommendations of International Ocean Colour Coordinating Group (IOCCG) (2013).

4.5. Exploiting temporal coherency

The temporal coherency of ocean colour data has rarely been exploited in ocean colour data processing. However, the extra benefits from high frequency geostationary may stimulate development of algorithms exploiting temporal coherency. Ocean colour remote sensing consists of viewing an ocean target that varies over timescales of hours to days through an atmosphere that varies much faster because of horizontal advection of clouds and aerosols. Ocean colour data processing is almost entirely performed on a pixel-by-pixel basis, yet it is sometimes concluded (Defoin Platel & Chami, 2007) that there may be insufficient radiometric information in a single pixel to perform an unambiguous inversion. For example, this may be seen as spatially noisy chlorophyll data in imagery, e.g. Figure 7 of Park, Van Mol, and Ruddick (2006). Ambiguous inversions may also occur for the atmospheric correction, for example, when different aerosol types/vertical distributions give aerosol reflectance that is identical in the near

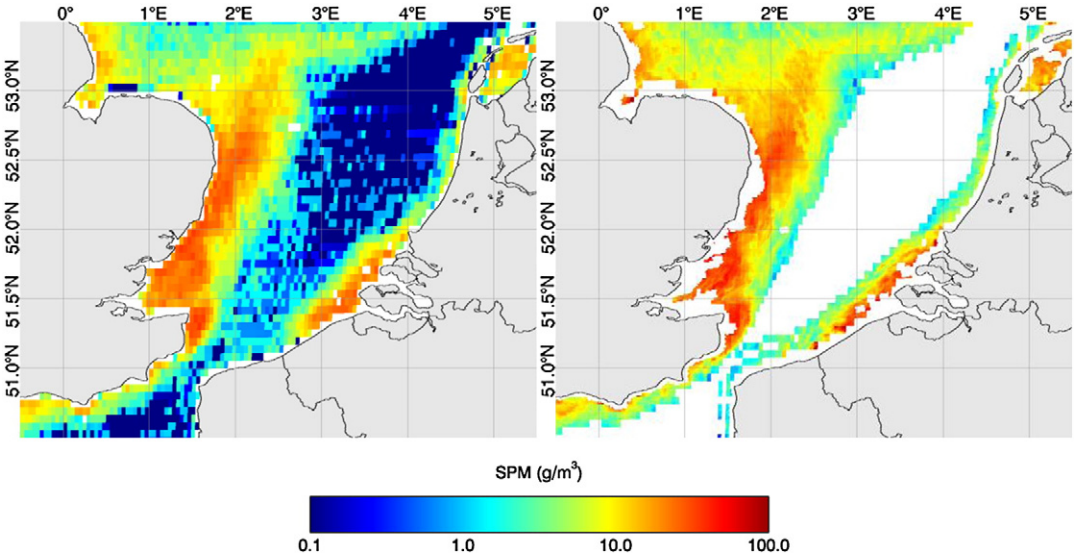

Fig. 11. Suspended particulate matter (SPM) concentration in the Southern North Sea at 10:45 UTC on 11 February 2008 from: (left) SEVIRI alone, (right) SEVIRI temporal modulation of the 12:45 overpass of MODIS-AQUA using the synergy algorithm of Vanhellemont et al. (2014–this volume). In the SEVIRI image areas with atmospheric correction failure and/or with the cloud mask set are masked in white. In the synergy SEVIRI/MODIS image, areas of clear water where the SEVIRI processing is expected to be sub-optimal, and areas with failure of the MODIS atmospheric correction or MODIS straylight flagging are given in white.
For full details of processing see Vanhellemont et al. (2014–this volume).

infrared but different in the blue. In such cases supplementary information may be of value in constraining the possible solution(s) to the inversion problem and suggestions have included the use of aerosol climatologies, with regional constraints on the vertical distribution of aerosols (Nobileau & Antoine, 2005). An alternative source of supplementary information for both the marine and the atmospheric inversion problems could be contained in the natural spatial and temporal coherency of marine processes.

For example, spatial homogeneity tests have long been used for the detection of clouds (McClain, Pichel, & Walton, 1985), which have much patchier distributions at kilometre scales than most marine parameters. Subjective identification of spatial inhomogeneities in an image is often used by scientists to spot obvious problems such as "noisy" chlorophyll distributions in turbid waters. More objectively, following from earlier work with SST imagery, empirical orthogonal function-based techniques can be used to automatically identify spatial outliers where a processing difficulty, e.g. cloud edge or shadow, has generated suspect data (Sirjacobs et al., 2011). In a similar way, temporal spikes can be identified in the post-processing of multitemporal ocean colour data and used to flag suspect or extreme data — a preliminary example of subjective identification of temporal spikes in early morning/late afternoon GOCI imagery, presumably associated with high air mass atmospheric correction difficulties, can be seen in Fig. 12. In this case, the multitemporal coefficient of variation over the day shows objectively the areas where erroneous data can be found in a single image. Such temporal spikes could be easily identified in automated post processing of ocean colour data using algorithms that are common in other scientific disciplines.

The way forward to exploitation of temporal coherency in the post L2 processing of ocean colour data is, thus, quite clear. Less clear is whether/how temporal coherency could be integrated in the L2 processing of ocean colour data, for example via probabilistic constraints on aerosol type or typical chlorophyll concentration based on recent/future retrievals. For example, viewing of the same target through different air masses over the day has already been proposed for geostationary remote sensing of aerosols over land (Knapp, Frouin, Kondragunta, & Prados, 2005). Current operational data processing chains have been strongly based on a traditional file structure of image-by-image (and then pixel-by-pixel) processing. However, after SeaWiFS had produced a few years of data, a growing user interest emerged for time series analysis of, for example, seasonal and interannual variability of chlorophyll. This led to a development of tools for visualising time series, such as GIOVANNI (Acker & Leptoukh, 2007). Advances in computer hardware mean that rapid and automated download and processing of full mission archives for local regions is now fast and simple (Vanhellemont & Ruddick, 2011) and L2 processing with information on adjacent pixels in time is quite feasible.

In a trivial preliminary example, the coarse sensor digitisation of the SEVIRI sensor, designed for imaging of much brighter targets, was found to be the main source of error on SPM products in clear waters. The signal:noise ratio was improved by simple moving-average filtering in time (Vanhellemont et al., 2014–this volume) of marine reflectance data before application of a turbidity retrieval algorithm.

4.6. Bidirectional effects

For locations with low diurnal variability of marine parameters, geostationary sensors provide an order of magnitude more information on the bidirectional reflectance of the ocean–atmosphere system because of the variation of sun angle over the day during cloud-free periods. Vanhellemont et al. (2014–this volume) show that measurements from a GEO over a day cover a wider range of scattering angles than is found for SSO and include situations of forward/side scattering. Bidirectionality of the marine reflectance has been studied primarily from the perspective of improving chlorophyll *a* retrieval in case 1 waters by correcting for variability associated with sun zenith angle (Morel & Gentili, 1993) and viewing angle (Morel & Gentili, 1996). Such model studies are confirmed by some rare in situ measurements of bidirectional reflectance (Voss, Morel, & Antoine, 2007) in case 1 waters. In both case 1 and case 2 waters (Loisel & Morel, 2001; Park & Ruddick, 2005), the particulate scattering phase function (SPF) is an important source of natural variability in the bidirectional response. The question then arises as to whether extra information on particles, going beyond just concentration e.g. to size distribution, could be extracted from measurements of bidirectional reflectance. Similarly in shallow waters, the bidirectional reflectance of the sea bottom may also impact water-leaving radiance, although this effect is often limited to a few percent (Mobley, Zhang, & Voss, 2003). At present it is unclear whether the second order variability of marine reflectance associated with sun angle variation over the day could be exploited or must be seen only as a factor to be corrected in algorithms for chlorophyll and SPM concentration retrievals. The potential for information extraction from bidirectional effects over the day will depend on the magnitude of the bidirectional variability as compared with other sources of variability in data, such as temporal variability of the target itself and uncertainty of the atmospheric correction, which will present a major challenge.

Going one step further, a dual view of the same location on earth from two geostationary sensors at different longitudes would give information on the bidirectional reflectance even for marine targets with diurnal variability and for stable targets would allow measurement of variability related both to sun angle and to viewing angle. Of course, the uncertainty of the atmospheric correction must again be kept sufficiently low to allow this variability to be quantified and it is possible that a dual view would provide more information on the atmosphere than

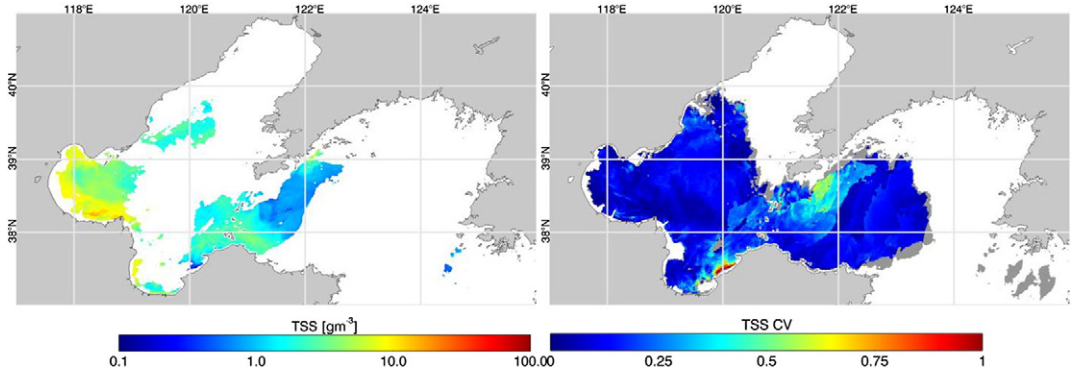

Fig. 12. GOCI-derived Total Suspended Solids (TSS) for the Bohai Sea (left) at 01:16 UTC, 12.6.2011, and (right) coefficient of variation (CV) over all cloud-free images of the same day. The areas of high CV over the day are caused mainly by apparently erroneous data in one or two images. In the right hand image pixels with zero/one data value for the day are given in white/grey respectively. Redrawn from Ruddick et al. (2012), which contains full details of processing and individual images used for composites. Reproduced with kind permission from Springer Science and Business Media © Springer.

on the ocean. Dual view geostationary remote sensing has not yet been attempted for ocean colour applications so it is difficult to foresee what improvements this will bring. However, it is noted that in SST remote sensing the dual view concept from a single satellite has been used on SSO sensors, starting with ATSR (Mutlow, Zavody, Barton, & Llewellyn-Jones, 1994), to enable a more accurate thermal infrared atmospheric correction and the multiple view capability of the POLDER sensor (Herman, Deuze, Marchant, Roger, & Lallart, 2005) has enabled an improvement in remote sensing of aerosols.

5. Conclusions and future perspectives

In this paper a review has been made of the early achievements in the field of geostationary ocean colour remote sensing and the potential impact of this new type of data on processing algorithms has been assessed.

The geostationary orbit offers the obvious advantage of greatly increased temporal resolution, and hence a higher probability of acquiring some data during days with scattered clouds. Since clouds are typically the number one obstacle to operational applications of ocean colour data that is already an important advantage. Equally obvious is the advantage, during cloud-free periods, of resolving fast processes relating to diurnal variability of biological processes or tidal variability. Thus, the critical problem of uncertainties in daily data from polar-orbiters related to unresolved temporal variability can be reduced (Lee et al., 2012). Moreover, the opportunity for extracting new information from the ocean, such as vertical migration of phytoplankton or information of diurnal variability of photosynthetic processes, has already been identified for geostationary remote sensing (IOCCG, 2012), based on high frequency in situ observations. These new possibilities are easy to see and, notwithstanding some algorithmic challenges, appear quite feasible. However, history suggests that the enormous increase in information that will come from geostationary ocean colour sensors is also likely to spawn entirely new ideas that cannot be foreseen here. Quoting (IOCCG, 2012), "this new way of observing the oceans is likely to generate unforeseen discoveries or entirely new ways of processing ocean-colour data. Just as the Coastal Zone Colour Scanner provided crucial first estimates of primary production for the world's oceans, far surpassing its planned one year mission and coastal zone focus, geostationary ocean colour is likely to provide information on unimagined new processes."

The geostationary orbit also presents new or more critical algorithmic challenges. Atmospheric correction algorithms will need to be improved for high zenith angle conditions to allow the full potential of geostationary ocean colour data to be exploited. Spatial resolution is severely cost-constrained and so the development of multi-sensor algorithms to combine the high temporal resolution of geostationary sensors with the typically higher spatial resolution of polar-orbiters may become important. The exploitation of temporal coherency for improving the quality or the quality control of ocean colour data becomes even more attractive with the high frequency data from geostationary sensors, and such algorithms are beginning to emerge, following in the footsteps of the SST remote sensing community. Finally the extra information on bidirectional reflectance provided by viewing a stable target over the day for different sun angles and (potentially) by dual viewing from geostationary sensors at different longitudes, provides a wealth of extra information on the ocean–atmosphere system which may be used to improve atmospheric correction and/or retrieval of extra marine parameters.

Whereas SSO have the distinct advantage for global applications of near-daily acquisition of data for the entire earth from a single sensor, the early successes of the GOCI mission raise questions about the optimal approach for ocean colour remote sensing of regional seas at tropical and temperature latitudes. The spectral resolution of GOCI is certainly limited, with only 8 visible/near infrared bands, none of the Short Wave Infrared bands that are important for turbid water atmospheric correction (Wang & Shi, 2005) and insufficient bands in the 660–710 nm range for optimal retrieval of chlorophyll absorption in turbid waters and of chlorophyll fluorescence. However, the spectral resolution of future geostationary sensors could clearly be improved. Considering that GOCI now provides ocean colour data at 500 m spatial resolution and an hourly temporal resolution for the Korea/China/Japan region, it is relevant to consider how SSO and GEO ocean colour sensors should be best combined in future for regional applications such as coastal water quality monitoring, harmful algae bloom detection, sediment transport and studying or monitoring the functioning of ecosystems.

Acknowledgements

This review was carried out in the framework of the GEOCOLOUR project, funded by the Belgian Science Policy Office STEREO programme under contract SR/00/139. Atmospheric correction at high zenith angle was reviewed under European Space Agency contract 4000107111/12/NL/AF. This review benefitted from discussions with the members of the IOCCG working group on geostationary ocean colour, including David Antoine and Jean-Loup Bézy, with the GEOCOLOUR steering committee including Youngje Park, Ewa Kwiatkowska and Hans Bonekamp, with the GOCI team at the Korea Ocean Satellite Center (KOSC) and with Marc Bouvet and Didier Ramon. EUMETSAT and the Royal Belgian Meteorological Institute (IRM/KMI) are acknowledged for supply of SEVIRI data. NASA is acknowledged for the supply of MODIS data. KOSC is acknowledged for the supply of GOCI data. Two anonymous reviewers are acknowledged for their careful reading of the text and their constructive comments.

References

Acker, J. G., & Leptoukh, G. (2007). Online analysis enhances use of NASA Earth science data. *Eos, Transactions of the American Geophysical Union*, *88*, 14.

Adams, C. N., & Kattawar, G. W. (1978). Radiative transfer in spherical shell atmosphere 1. Rayleigh scattering. *Icarus*, *35*, 139–151.

Ahn, J. H., Park, Y. -J., Ryu, J. -H., Lee, B., & Oh, I. S. (2012). Development of atmospheric correction algorithm for Geostationary Ocean Color Imager (GOCI). *Ocean Science Journal*, *47*, 247–260.

Barnes, R. A., Eplee, R. E., Schmidt, G. M., Patt, F. S., & McClain, C. R. (2001). Calibration of SeaWiFS. I. Direct techniques. *Applied Optics*, *40*, 6682–6700.

Beckers, J. M., & Rixen, M. (2003). EOF calculations and data filling from incomplete oceanographic datasets. *Journal of Atmospheric and Oceanic Technology*, *20*, 1839–1856.

Bresciania, Mariano, Stroppiana, D., Odermatt, D., Morabito, G., & Giardino, C. (2011). Assessing remotely sensed chlorophyll-a for the implementation of the Water Framework Directive in European perialpine lakes. *Science of the Total Environment*, *409*, 3083–3091.

Bruyant, F., Babin, M., Genty, F., Prasil, O., Behrenfeld, M. J., Claustre, H., et al. (2005). Diel variations in the photosynthetic parameters of *Prochlorococcus* strain PCC 9511: Combined effects of light and cell cycle. *Limnology and Oceanography: Methods*, *50*, 850–863.

Choi, J. -K., Park, Y. J., Ahn, J. H., Lim, H. -S., Eom, J., & Ryu, J. -H. (2012). GOCI, the world's first geostationary ocean color observation satellite, for the monitoring of temporal variability in coastal water turbidity. *Journal of Geophysical Research*, *117*.

Choi, J. -K., Park, Y. -J., Lee, B. R., Eom, J., Moon, J. -E., & Ryu, J. -H. (2014). Application of the Geostationary Ocean Color Imager (GOCI) to mapping of temporal dynamics of coastal water turbidity. *Remote Sensing of Environment*, *146*, 24–35 (this volume).

Choi, J. -K., Yang, H., Han, H. -J., Ryu, J. -H., & Park, Y. -J. (2013). Quantitative estimation of suspended sediment movements in coastal region using GOCI. *Journal of Coastal Research Special Issue*, *65*, 1367–1372.

Defoin Platel, M., & Chami, M. (2007). How ambiguous is the inverse problem of ocean color in coastal waters. *Journal of Geophysical Research*, *112*. http://dx.doi.org/10.1029/2006JC003847.

Desmit, X., Vanderborght, J. -P., Regnier, P., & Wollast, R. (2005). Control of phytoplankton production by physical forcing in a strongly tidal, well-mixed estuary. *Biogeosciences*, *2*, 205–218.

Ding, K., & Gordon, H. R. (1994). Atmospheric correction of ocean-color sensors: Effects of the Earth's curvature. *Applied Optics*, *33*, 7096–7106.

Doerffer, R., & Fischer, J. (1994). Concentrations of chlorophyll, suspended matter, gelbstoff in case II waters derived from satellite coastal zone color scanner data with inverse modeling methods. *Journal of Geophysical Research*, *99*, 7457–7466.

Doxaran, D., Lamquin, N., Park, Y. -J., Mazeran, C., Ryu, J. -H., Wang, M., et al. (2014). Retrieval of the seawater reflectance for suspended solids monitoring in the East China Sea using MODIS, MERIS and GOCI satellite data. *Remote Sensing of Environment*, *146*, 36–48 (this volume).

Ehlers, M. (1991). Multisensor image fusion techniques in remote sensing. *ISPRS Journal of Photogrammetry and Remote Sensing*, *46*, 19–30.

Franz, B.A., Bailey, S. W., Werdell, P. J., & McClain, C. R. (2007). Sensor independent approach to the vicarious calibration of satellite ocean color radiometry. *Applied Optics*, *46*, 5068–5082.

Freitas, S.C., Trigo, I. F., Macedo, J., Barroso, C., Silva, R., & Perdigao, R. (2013). Land surface temperature from multiple geostationary satellites. *International Journal of Remote Sensing*, *34*, 3051–3068.

Frouin, R., & McPherson, J. (2012). Estimating photosynthetically available radiation at the ocean surface from GOCI data. *Ocean Science Journal*, *47*, 312–322.

Fu, G., Baith, K. S., & McClain, C. R. (1998). SeaDAS: The SeaWiFS data analysis system. *4th Pacific Ocean remote sensing conference* (pp. 73–79). Qingdao, China: Remote Sensing Institute, Qingdao.

Gordon, H. R. (1978). Removal of atmospheric effects from satellite imagery of the oceans. *Applied Optics*, 1631–1636.

Gordon, H. R., Brown, J. W., & Evans, R. H. (1988). Exact Rayleigh scattering calculations for use with the Nimbus-7 Coastal Zone Color Scanner. *Applied Optics*, *27*, 862–871.

Gordon, H. R., & Morel, A. Y. (1983). Remote assessment of ocean color for interpretation of satellite visible imagery. New York: Springer-Verlag.

Gordon, H. R., & Wang, M. (1994). Retrieval of water-leaving radiance and aerosol optical thickness over the oceans with SeaWiFS: A preliminary algorithm. *Applied Optics*, *33*, 443–452.

Govaerts, Y. M., Lattanzio, A., Taberner, M., & Pinty, B. (2008). Generating global surface albedo products from multiple geostationary satellites. *Remote Sensing of Environment*, *112*, 2804–2816.

He, X., Bai, Y., Pan, D., Huang, N., Dong, X., Chen, J., et al. (2013). Using geostationary satellite ocean color data to map the diurnal dynamics of suspended particulate matter in coastal waters. *Remote Sensing of Environment*, *133*, 225–239.

Herman, M., Deuze, J. L., Marchant, A., Roger, B., & Lallart, P. (2005). Aerosol remote sensing from POLDER/ADEOS over the ocean: Improved retrieval using a nonspherical particle model. *Journal of Geophysical Research*, *110*.

Hong, G. H., Yang, D. B., Lee, H. -M., Yang, S. R., Chung, H. W., Kim, C. J., et al. (2012). Surveillance of water disposal activity at sea using satellite ocean color imagers: GOCI and MODIS. *Ocean Science Journal*, *47*, 387–394.

Hooker, S. B., & McClain, C. R. (2000). The calibration and validation of SeaWiFS data. *Progress in Oceanography*, *45*, 427–465.

Hu, C., Chen, Z., Clayton, T. D., Swarzenski, P., Brock, J. C., & Muller-Karger, F. E. (2004). Assessment of estuarine water-quality indicators using MODIS medium-resolution bands: Initial results from Tampa Bay, FL. *Remote Sensing of Environment*, *93*, 423–441.

International Ocean Colour Coordinating Group (IOCCG) (1998). In A. Morel (Ed.), *Minimum requirements for an operational, ocean colour sensor for the open ocean*. IOCCG Report No.1: 50.

International Ocean Colour Coordinating Group (IOCCG) (2007). In W. W. Gregg (Ed.), *Ocean colour data merging*. IOCCG Report No.6: 68.

International Ocean Colour Coordinating Group (IOCCG) (2010). In M. Wang (Ed.), *Atmospheric correction for remotely-sensed ocean colour products*. IOCCG Report No.10: 78.

International Ocean Colour Coordinating Group (IOCCG) (2012). In D. Antoine (Ed.), *Ocean Colour observations from a geostationary orbit*. IOCCG Report No.12: 102.

International Ocean Colour Coordinating Group (IOCCG) (2013). In C. R. McClain, & G. Meister (Eds.), *Mission Requirements for Future Ocean-Colour Sensors*. IOCCG Report No.13: 115.

Kamykowski, D. (1981). Laboratory experiments on the diurnal vertical migration of marine dinoflagellates through temperature gradients. *Marine Biology*, *62*, 57–64.

Knapp, K. E., Frouin, R., Kondragunta, S., & Prados, A. I. (2005). Towards aerosol optical depth retrievals over land from GOES visible radiances: Determining surface reflectance. *International Journal of Remote Sensing*, *26*(18), 4097–4116.

Knapp, K. R., Ansari, S., Bain, C. L., Bourassa, M.A., Dickinson, M. J., Funk, C., et al. (2011). Globally gridded satellite (GridSat) observations for climate studies. *Bulletin of the American Meteorological Society*, *92*, 893–907. http://dx.doi.org/10.1175/2011BAMS3039.1.

Lee, Z., Jiang, M., Davis, C., Pahlevan, N., Ahn, Y. -H., & Ma, R. (2012). Impact of multiple satellite ocean color samplings in a day on assessing phytoplankton dynamics. *Ocean Science Journal*, *47*, 323–329.

Loisel, H., & Morel, A. (2001). Non-isotropy of the upward radiance field in typical coastal (Case 2) waters. *International Journal of Remote Sensing*, *22*, 275–295.

Loisel, H., Vantrepotte, V., Nordkvist, K., Mériaux, X., Kheireddine, M., Ras, J., et al. (2011). Characterization of the bio-optical anomaly and diurnal variability of particulate matter, as seen from scattering and backscattering coefficients, in ultra-oligotrophic eddies of the Mediterranean Sea. *Biogeosciences*, *8*, 3295–3317.

McClain, C. R. (2009). A decade of satellite ocean color observations. *Annual Review of Marine Science*, *1*, 19–42.

McClain, E. P., Pichel, W. G., & Walton, C. C. (1985). Comparative performance of AVHRR-based multichannel sea surface temperature. *Journal of Geophysical Research*, *90*, 11589–11601.

Miller, R. L., & McKee, B.A. (2004). Using MODIS Terra 250 m imagery to map concentrations of total suspended matter in coastal waters. *Remote Sensing of Environment*, *93*, 259–266.

Mobley, C. D. (1994). Light and water: Radiative transfer in natural waters. London: Academic Press.

Mobley, C. D., Zhang, H., & Voss, K. J. (2003). Effects of optically shallow bottom on upwelling radiances: Bidirectional reflectance distribution function effects. *Limnology and Oceanography*, *48*, 337–345.

Morel, A., & Gentili, B. (1993). Diffuse reflectance of oceanic waters II. Bidirectional aspects. *Applied Optics*, *32*, 6864–6879.

Morel, A., & Gentili, B. (1996). Diffuse reflectance of oceanic waters. III. Implications of bidirectionality for the remote sensing problem. *Applied Optics*, *35*, 4850–4862.

Morel, A., & Maritorena, S. (2001). Bio-optical properties of oceanic waters: A reappraisal. *Journal of Geophysical Research*, *106*, 7163–7180.

Morel, A., & Prieur, L. (1977). Analysis of variations in ocean color. *Limnology and Oceanography*, *22*, 709–722.

Mutlow, C. T., Zavody, A.M., Barton, I. L., & Llewellyn-Jones, D. T. (1994). Sea surface temperature measurements by the along-track scanning radiometer on the ERS-1 satellite: Early results. *Journal of Geophysical Research*, *99*, 22575–22588.

Neukermans, G. (2012). Optical in situ and geostationary satellite-borne observations of suspended particles in coastal waters. *Ph.D. dissertation, Université du Littoral Côte d'Opale, France*. Brussels, Belgium: Academic and Scientific Publishers. ISBN 978 90 7028 949 2 (Perma-link: http://www2.mumm.ac.be/downloads/publications/neukermans_phd_manuscript_a4.pdf)

Neukermans, G., Ruddick, K., Bernard, E., Ramon, D., Nechad, B., & Deschamps, P. -Y. (2009). Mapping total suspended matter from geostationary satellites: a feasibility study with SEVIRI in the Southern North Sea. *Optics Express*, *17*, 14029–14052.

Neukermans, G., Ruddick, K., & Greenwood, N. (2012). Diurnal variability of turbidity and light attenuation in the southern North Sea from the SEVIRI geostationary sensor. *Remote Sensing of Environment*, *124*, 564–580.

Nobileau, D., & Antoine, D. (2005). Detection of blue-absorbing aerosols using near infrared and visible (ocean color) remote sensing observations. *Remote Sensing of Environment*, *95*, 368–387.

Park, Y., & Ruddick, K. (2005). Model of remote-sensing reflectance including bidirectional effects for case 1 and case 2 waters. *Applied Optics*, *44*, 1236–1249.

Park, Y., Van Mol, B., & Ruddick, K. (2006). Validation of MERIS water products for Belgian coastal waters: 2002–2005. In D. Danesy (Ed.), *Second working meeting on MERIS and AATSR calibration and geophysical validation (MAVT-2006)*. ESA.

Robinson, I. (2004). Measuring the oceans from space: The principles and methods of satellite oceanography. Berlin: Springer.

Ruddick, K., Vanhellemont, Q., Yan, J., Neukermans, G., Wei, G., & Shang, S. (2012). Variability of suspended matter in the Bohai Sea from the Geostationary Ocean Color imager (GOCI). *Ocean Science Journal*, *47*, 331–345.

Ryu, J. -H., Han, H. -J., Cho, S., Park, Y. -J., & Ahn, Y. -H. (2012). Overview of Geostationary Ocean Color Imager (GOCI) and GOCI Data PRocessing System (GDPS). *Ocean Science Journal*, *47*, 223–233.

Ryu, J. -H., & Ishikaza, J. (2012). GOCI data processing and ocean applications. *Ocean Science Journal*, *47*, 221.

Santer, R., & Schmechtig, C. (2000). Adjacency effects on water surfaces: Primary scattering approximation and sensitivity study. *Applied Optics*, *39*, 361–375.

Sanwlani, N., Chauhan, P., & Navalgund, R. R. (2011). Dust storm detection and monitoring using multi-temporal INSAT-3A-CCD data. *International Journal of Remote Sensing*, *32*, 5527–5539.

Schmetz, J., Pili, P., Tjemkes, S., Just, D., Kerkmann, J., Rota, S., et al. (2002). An introduction to METEOSAT Second Generation (MSG). *Bulletin of the American Meteorological Society*, 977–992.

Shaw, G. E. (1983). Sun photometry. *Bulletin of the American Meteorological Society*, *64*, 4–10.

Sirjacobs, D., Alvera-Azcárate, A., Barth, A., Lacroix, G., Park, Y., Nechad, B., et al. (2011). Cloud filling of ocean color and sea surface temperature remote sensing products over the Southern North Sea by the Data Interpolating Empirical Orthogonal Functions methodology. *Journal of Sea Research*, *65*, 114–130.

Spurr, R. J.D. (2002). Simultaneous derivation of intensities and weighting functions in a general pseudo-spherical discrete ordinate radiative transfer treatment. *Journal of Quantitative Spectroscopy and Radiative Transfer*, *75*, 129–175.

Sterckx, S., Knaeps, E., & Ruddick, K. (2011). Detection and correction of adjacency effects in hyperspectral airborne data of coastal and inland waters: The use of the near infrared similarity spectrum. *International Journal of Remote Sensing*, *32*, 6470–6505.

Stramska, M., & Dickey, T. D. (1992). Variability of bio-optical properties of the upper ocean associated with diel cycles in phytoplankton population. *Journal of Geophysical Research*, *97*, 17873–17887.

Stumpf, R. P., Gelfenbaum, G., & Pennock, J. R. (1993). Wind and tidal forcing of a buoyant plume, Mobile Bay, Alabama. *Continental Shelf Research*, *13*, 1281–1301.

Vanhellemont, Q., Neukermans, G., & Ruddick, K. (2014). Synergy between polar-orbiting and geostationary sensors: Remote sensing of the ocean at high spatial and high temporal resolution. *Remote Sensing of Environment*, *146*, 49–62 (this volume).

Vanhellemont, Q., & Ruddick, K. (2011). Generalized satellite image processing: Eight years of ocean colour data for any region on earth. *Proceedings of the SPIE remote sensing conference, Prague*.

Voss, K. J., Morel, A., & Antoine, D. (2007). Detailed validation of the bidirectional effect in various Case 1 waters for application to ocean color imagery. *Biogeosciences*, *4*, 781–789.

Wang, M. (2003). Light scattering from the spherical shell atmosphere: Earth curvature effects measured by SeaWiFS. *Eos, Transactions of the American Geophysical Union*, *84*, 529 (530, 534).

Wang, M. (2006). Effects of ocean surface reflectance variation with solar elevation on normalized water-leaving radiance. *Applied Optics*, *45*, 4122–4128.

Wang, M., & Shi, W. (2005). Estimation of ocean contribution at the MODIS near-infrared wavelengths along the east coast of the U.S.: Two case studies. *Geophysical Research Letters*, *32*.

Yang, C. -S., & Song, J. -H. (2012). Geometric performance evaluation of the Geostationary Ocean Color Imager. *Ocean Science Journal*, *47*, 235–246.

Zibordi, G., Holben, B., Slutsker, I., Giles, D., D'Alimonte, D., Mélin, F., et al. (2009). AERONET-OC: A network for the validation of ocean color primary product. *Journal of Atmospheric and Oceanic Technology*, *26*, 1634–1651.